Complexities of splashing

R.D. Deegan*, P. Brunet †, and J. Eggers †

* Department of Physics and Center for the Study of Complex Systems, Randall Laboratory, University of Michigan, Ann Arbor, MI 48109, USA.
†School of Mathematics, University of Bristol, University Walk, Bristol BS8 1TW, United Kingdom.

Abstract. We study the impact of a drop of liquid onto a thin layer of the same liquid. We give an overview of the sequence of events that occur as the two most important dimensionless control parameters are varied. In particular, multiple cohorts of droplets can be ejected at different stages after impact due to different mechanisms. Edgerton's famous *Milkdrop Coronet* is only observed for a narrow range of parameters. Outside of this range, the splash is either qualitatively different, or suffers from a much lower level of regularity.

1. Introduction

The ubiquity of splashes, caused by the collision of a fluid drop with a surface, has been argued eloquently by Worthington [1]. Indeed, splashes are one of the main fascinations of fluid mechanics [2]. The detailed sequence of events following impact depends very much on the speed and the type of fluid, but also on the substrate. If the substrate is dry, results depend on the smoothness of the surface [3], the wetting angle between solid and liquid [4], and the presence of air [5]. Impact may be into a deep pool of the same liquid [1], or onto a thin layer of the same [6, 7, 8] or another liquid [9]. Non-Newtonian liquid behaviour can also change the result qualitatively [10, 11].

Harold Edgerton [6] discovered that the impact onto a thin layer results in the most regular structure, the famous *Milkdrop Coronet*. Similar crowns, albeit more disordered, had been found earlier by Worthington when studying impact on a deep pool [12]. As illustrated in Fig. 1, Edgerton lets a sequence of milk drops fall onto a solid surface to establish a thin layer of liquid. In this paper, by contrast, we carefully control the thickness of the target fluid layer. However, as pointed out by Kadanoff [13], and as illustrated by the cover of this issue and in Fig. 2, not all events have the same degree of regularity. There are also indications that the regularity seen in Edgerton's photograph arises from the non-Newtonian properties of milk which help to damp perturbations [14].

In this paper we illustrate that the regular crown structure found by Edgerton is a

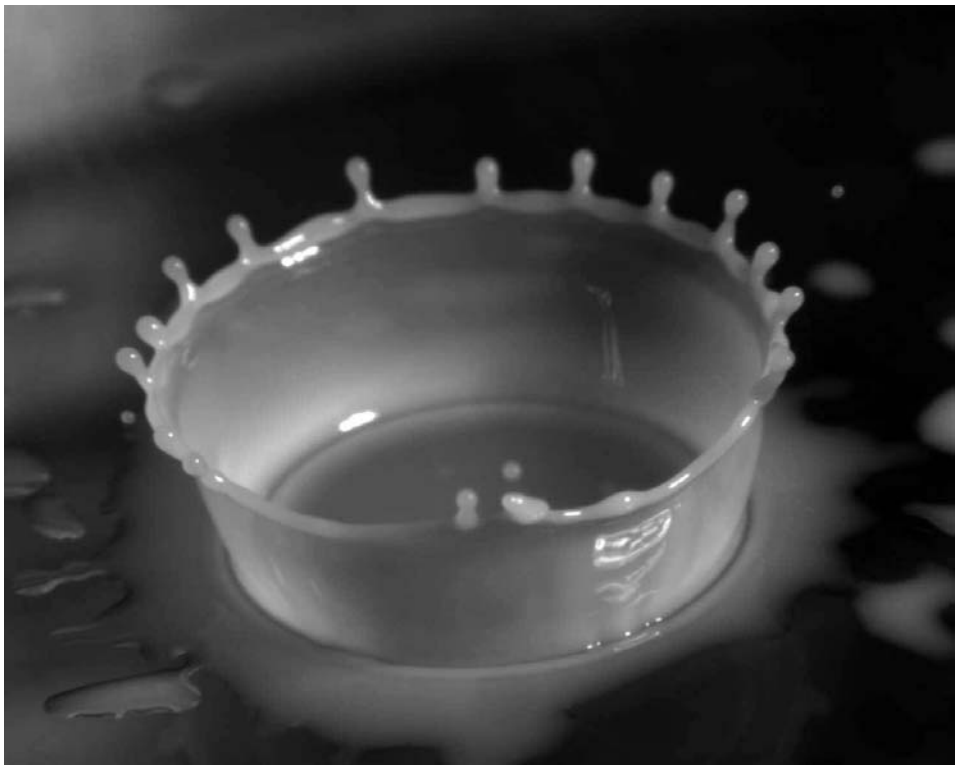

Figure 1. A sequence of milk drops falling on a solid surface.

rare exception, observed only in a narrow range of parameters. As we will show in more detail below, the formation of an Edgerton milk crown results from an intricate sequence of events. First, a cylindrical fluid sheet shoots out from the layer, forming a fat rim. Second, cylindrical symmetry is broken by a linear instability of the rim, which selects a preferred wavelength at which the thickness of the rim varies periodically. Third, in a nonlinear stage of the original instability, the rim develops tips, from which jets emanate. Fourth, drops pinch off from the end of each jet. Irrespective of its regularity, we herein call the generation of droplets by this mechanism a **crown splash**.

In practise, a whole range of other phenomena can take place as one moves outside the light shaded region of Fig. 3. In particular, there are at least two separate mechanisms by which sheets form upon impact, and the end products of the impact event are strongly influenced by whether these sheets decay separately, commingle, or interact. The symmetry breaking instability of each sheet may occur by one or more mechanisms, leading to noisy structures in general.

Our study is meant to elucidate the complexities of drop impact onto a thin layer, by pointing out the existence of different structures in different ranges of the space of control parameters. Failing that, it is impossible to appreciate the distinct dynamical origins of secondary droplets.

To a very good approximation, our experiments represent a spherical drop of a Newtonian liquid, of diameter D, impacting with velocity U onto a fluid layer of thickness h of the same liquid. For all our experiments, h is fixed at $0.2D$. More details of possible deviations from a spherical shape, influence of air, etc. are discussed

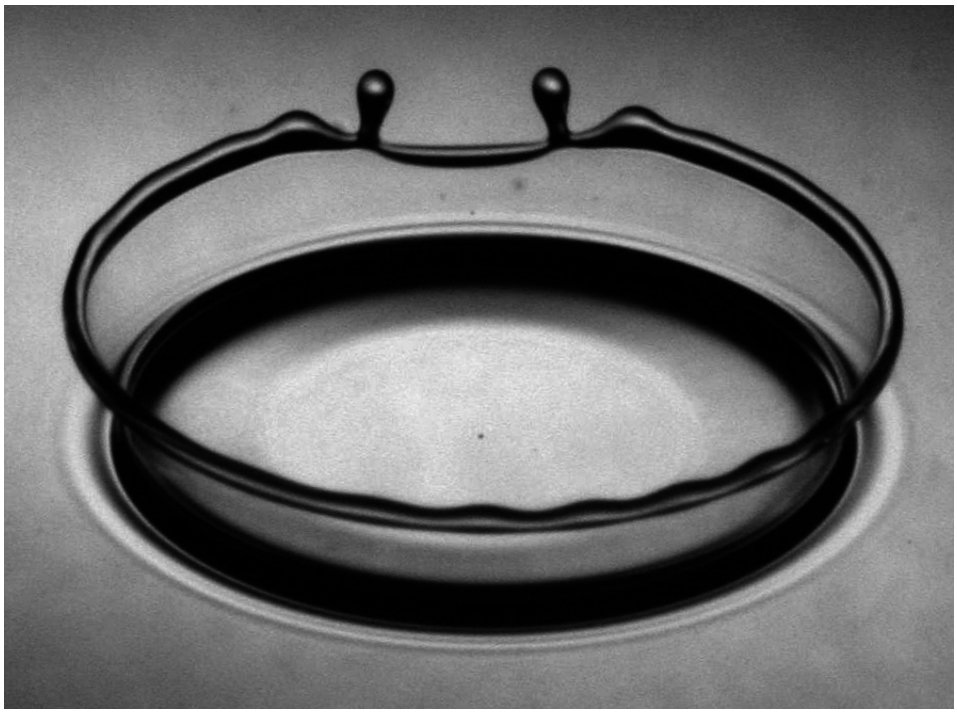

Figure 2. Impact of propanol drop on the same fluid.

in the experimental section.

Conventional dimensionless parameters are the Weber number, Reynolds number, Froude number, and the dimensionless thickness of the layer:

$$\mathsf{We} = \frac{\rho D U^2}{\gamma}, \quad \mathsf{Re} = \frac{DU}{\nu}, \quad \mathsf{Fr} = \frac{U^2}{gD}, \quad \mathsf{H} = \frac{h}{D}. \tag{1}$$

The most important parameters are the Weber number (We) and the Reynolds number (Re). Gravity is negligible as indicated by the typical Froude number of 10^2, and we will therefore disregard it. The layer thickness h plays a small role on a quantitative level, but does not affect things qualitatively, as long as one stays within the realm of thin layers.

2. Experiments

In our experiments a drop was produced from a beveled hypodermic needle (gauge 21, 26, or 30) held at a fixed height 20-120 cm above a liquid bath, as shown in Fig. 4.

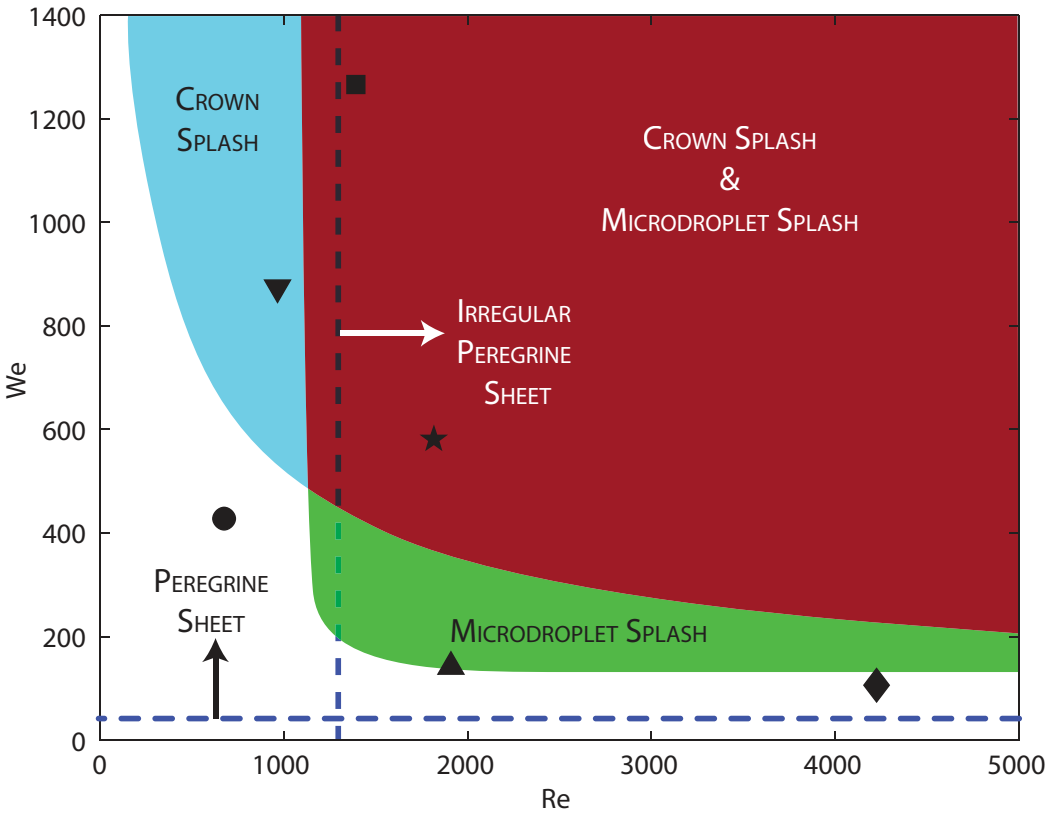

Figure 3. Phase diagram indicating the qualitatively different regimes of drop impact. The dashed vertical line indicates the Re beyond which the Peregrine sheet is disordered, and the horizontal dashed line indicates the We number above which a Peregrine sheet forms.

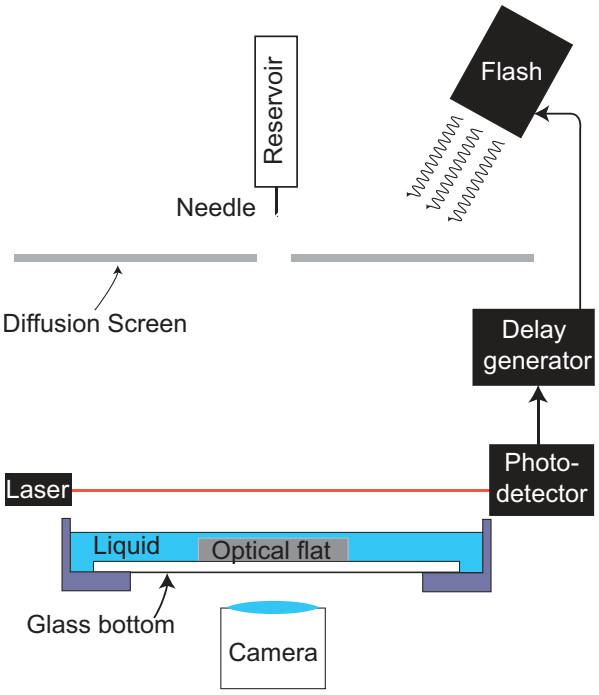

Figure 4. Experimental apparatus.

The needle was gravity fed from an open reservoir. The waiting time between two drop impacts was set to be more than 10 seconds, to allow the layer to recover a flat horizontal shape. The target layer was formed in the bath between the liquid surface and a 4 inch diameter, $\lambda/4$, glass, optical flat (Edmund Optics). The bottom of the bath was also glass, permitting an unimpeded view of the impact from below. The layer depth was measured using a needle mounted on a micrometer to locate the liquid surface and the solid substrate. Depending on the drop size this ranged from 290-580 μm, and was uniform to within ± 10 μm.

Images were acquired with either a high speed video camera (Phantom 5.0, Vision Research Inc.) or with a still camera (Canon 20D SLR). Back-lighting was used through out and provided by two 500W halogen lamps for filming or by a 6 Joule, 500 ns flash (Palflash 501, Pulse Photonics Ltd.). The flash was triggered by the drop cutting a collimated laser sheet focused onto a photo-detector. A home-made delay generator enables us to take pictures at a desired time after impact. The reproducibility of the image capture was ± 10 μs. Due to the back-lighting the drop obscured the earliest times after impact. The high speed video camera was typically set to capture a 10 μs exposure, with a resolution of 512 x 256 pixels at 7,400 frames per second. The advantage of taking single flash photographs was the much improved spatial and temporal resolution.

We used propanol, water, silicon oil, and a 32/68 w/w mixture of glycerol and water. The values for the fluid properties used to calculate Re and We are given in Table 1. The diameter of the drops was calculated from the weight of the drops, and the speed of the drop before impact was measured from video footage. Drops with diameters 1.4-2.9 mm were generated using different gauge needles. For all drop sizes

the oscillations caused by the drop pinch died off quickly. For larger drops, though, the leading surface of the drop was flattened by air drag. Except just prior to impact, drops smaller than 2.0 mm were spherical to within our capacity to measure. At impact all drops develop a small concavity on the leading surface due to the strong lubrication pressure as air is squeezed out from between the drop and the impact layer [15]. The speed at impact was increased by raising the fall height, and was noticeably slowed by air drag.

3. Two types of sheets

There are at least two types of sheets, of completely different physical origin, produced when the drop hits the fluid layer. We will discuss them in turn.

3.1. Ejecta sheet

This sheet, first observed experimentally by Thoroddsen [15] and seen in numerical simulations by [16] is produced at the moment of impact. An example is shown in Fig. 5. As the drop touches the surface at finite speed, a localised pressure singularity is produced, pushing fluid outward. From the symmetry of the problem at the first moment of impact it is clear that the sheet must shoot out horizontally, and that an equal amount of drop and layer fluid is contained in it.

A theory of the ejecta sheet was presented in [17], neglecting both surface tension and viscosity. Thus both the Reynolds and Weber numbers are infinite. In this limit, there is no time scale to the problem, and the sheet instantaneously reaches infinity. As the drop penetrates the layer, the sheet thickens and a larger percentage comes from the layer fluid. Clearly, in reality the ejecta sheet cannot shoot out to infinity, and certainly not in zero time; restoring surface tension to the problem, as was done in simulations of [16], yields a finite speed (see Figs. 4-6 in [16]). Ejecta sheet speeds were measured experimentally by [15], and show increasingly high speeds with decreasing viscosity, reaching up to 50 m/s.

Weiss and Yarin [16] also investigate the role of surface tension for the *existence* of an ejecta sheet. They find that for $\mathsf{We} < 40$ no ejecta sheet is produced at all. Rather, the motion is transformed into a capillary wave that runs along the drop. In

Table 1. Properties of fluids used in our experiments.

Fluid	ρ (g/cm^3)	η (cP)	γ (dynes/cm)
Water	1.00	1.0	75
Propanol	0.79	2.4	23
Silicon oil	0.92	5.2	21
Glycerol/water mixture	1.08	2.9	73

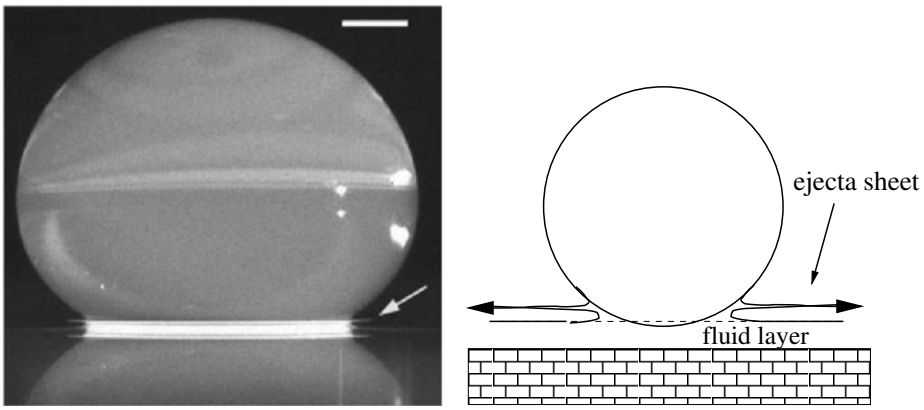

(a) (b)

Figure 5. *Left:* An experimental snapshot of a drop directly after impact [15]. The parameters are $\mathsf{Re} = 1080, \mathsf{We} = 4170$. *Right:* A cartoon of the same process, following [17]. An ejecta sheet shoots out horizontally from underneath the drop.

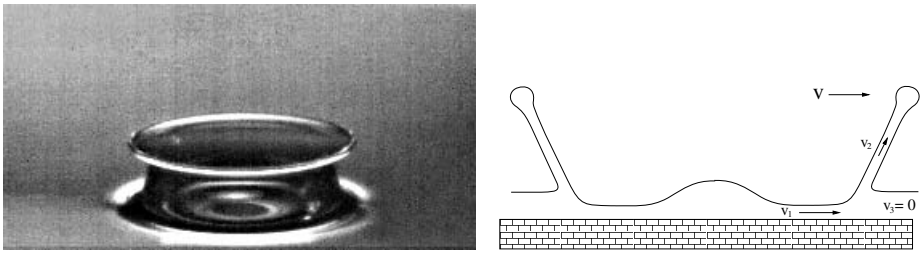

(a) (b)

Figure 6. *Left:* an experiment corresponding to the cartoon on the right. The parameters are $\mathsf{Re} = 676, \mathsf{We} = 428$, 775 μs after impact. Corresponds to • in Fig. 3. Right: A cartoon of the mechanism for sheet formation as proposed in [2]. Mass and momentum conservation determine the velocity and angle of the upward moving sheet, which usually rises at a steep angle.

our experiments, we observe small droplets long before the crown splash but we do not have the resolution to observe the mechanism by which these are generated. On our phase diagram, all such cases are lumped together with the label **microdroplet splash**. Nonetheless, if we assume that these microdroplets originate in the breakup of the ejecta sheet then our boundary at high Re approaches $\mathsf{We} = 130$ in fair agreement with Weiss and Yarin's result of $\mathsf{We} \approx 40$ for $\mathsf{Re} \to \infty$.

3.2. Peregrine sheet

After the drop has penetrated the layer, a sheet of liquid travels outward over the solid surface. It collides head on with the as-yet unmixed fluid in the preexisting layer. This mechanism, first described by Peregrine [2], is illustrated in Fig. 6. Elementary considerations of mass and momentum balance shows that, given the thicknesses and

Figure 7. An ejecta sheet "riding" on a Peregrine sheet. The former leads to the formation of tiny droplets that precede the much larger Peregrine sheet. Re=1354, We=874, 580 μs after impact. Corresponds to ★ in Fig. 3.

velocities of the two incoming sheets (in the frame of reference of the moving base), that the speed, thickness and ejection angle of the resulting sheet can be calculated. An experimental example is shown in Fig. 6. Peregrine sheets form for $\mathsf{We} > 40$, and are disordered from the earliest observable times for $\mathsf{Re} > 1300$. These features are respectively denoted by a dashed horizontal and vertical line in Fig. 3.

3.3. Combination of two sheets

This qualitative breakdown of the splash is summarized in Fig. 3. For most of the parameter regime of our experiments, the two sheets described appear together in any given impact event. We are aware of three different fates of the ejecta sheet.

(i) The ejecta sheet becomes the leading edge of the Peregrine sheet, as the latter grows underneath the former. In Fig. 7 we show a Peregrine sheet, whose rim has not yet broken up. Yet a number of very small drops precede the rim. These form from a horizontal sheet attached to the rim at early times.

(ii) The ejecta sheet collides with the fluid layer, trapping pockets of air in substrate liquid. We have observed a circular residue of bubbles surrounding the impact center that persist long after impact. Weiss and Yarin [16] observe this process in their numerical calculations.

(iii) The ejecta sheet breaks up immediately (the so-called **prompt splash**; see Fig. 8). This may lead to additional irregularity of the Peregrine sheet and kick start the rim instability.

4. Symmetry breaking

The initial configuration is cylindrically symmetric, yet most final configurations break this symmetry. This indicates the existence of one or more instabilities, which break the

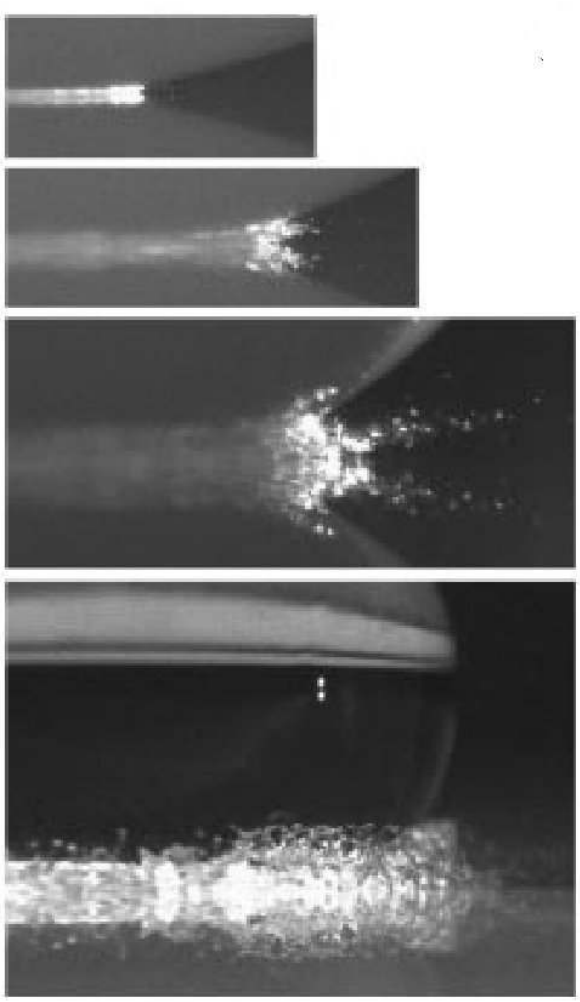

Figure 8. A ejecta sheet breaking up into many smaller droplets, at a stage where the sheet is still hidden completely underneath the drop [15]. The parameters are $\mathsf{Re} = 2.9 \times 10^4$ and $\mathsf{We} = 1.8 \times 10^3$.

symmetry. This is surely the case for the prompt splash shown in Fig. 8, which suggests almost instantaneous breakup into many very small droplets. There may be many more instabilities associated with the ejecta sheet, but we will not elaborate here, since we have little original data to report.

We begin by remarking that the symmetry is not *necessarily* broken, at least not to a degree that is measurable experimentally. An example of this situation is shown in the series of panels of Fig. 9(left). A Peregrine sheet develops a rim, but even as the rim falls back into the layer, no instability is observed.

A different variant of the same situation is seen on the right of the same figure, for an impact that takes place at much higher Re (see the phase diagram in Fig. 3). Although the rim never breaks up, the flow is irregular from the earliest times of observation. A possible explanation is that the high Reynolds number introduces turbulence into the flow.

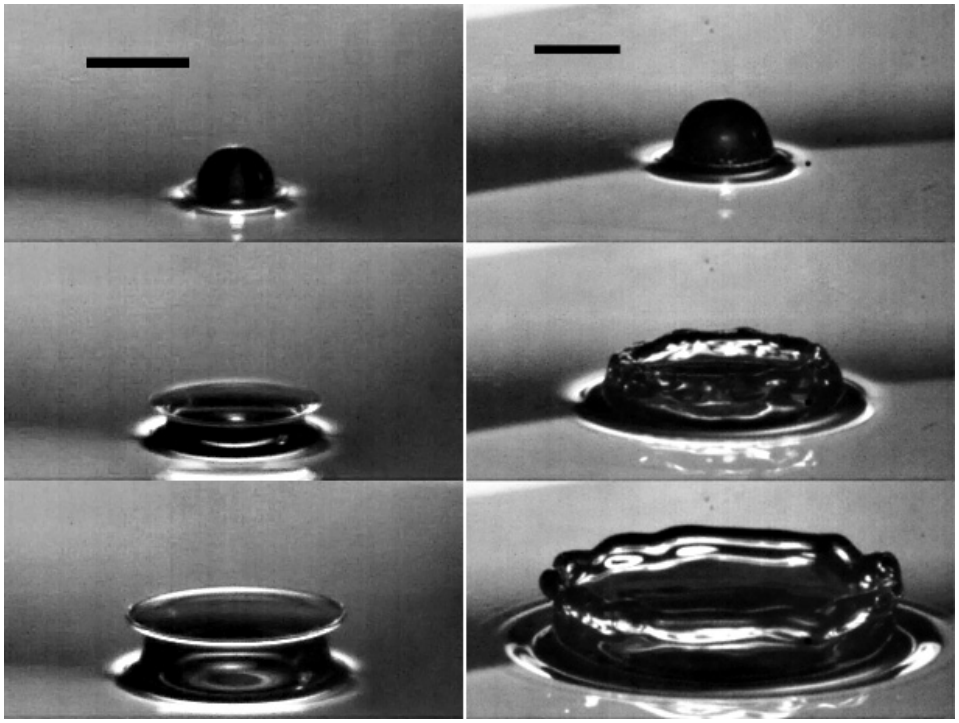

Figure 9. Smooth and disordered Peregrine sheets that do not produce secondary droplets. *Left:* Silicon oil, Re=676, We=428, H = 0.2 at 100, 368, 775 μs after impact. Corresponds to circle in Fig. 3. *Right:* Water Re=4226, We=106, H = 0.2 at 300, 1650, 4215 μs after impact. Corresponds to ♦ in Fig. 3. Scale bar corresponds to 2 mm.

The sequence in Fig. 10 *left* corresponds to Edgerton's crown (Fig.1) described above. First, a Peregrine sheet is formed, which only turns unstable at its rim, owing to a varicose instability. The wavelength selection associated with this Rayleigh-Plateau instability will be investigated in more detail in a future publication. Note in particular that fluctuations in the local wavelength remain as one goes around the rim.

As the perturbations grow in size, modest local variations of the rim radius turn into spikes, pointing away from the sheet. We have confirmed that apart from a slight coarsening (merging of two spikes), the initial linear instability sets the number of tips (jets) on the crown. Most jets shed a drop from their end, so the initial instability is also crucial for the determination of the number of drops.

On the right of Fig. 10 drops are produced as well, but of a far smaller size. The rim of the Peregrine sheet develops an instability, but doesn't grow enough to lead to drops. However, drops have been produced close to the moment of impact. We suspect the process of drop formation is analogous to what is shown in Fig. 8. Thus the drops seen in the later stages of the sheet formation in Fig. 10 (right) are simply a remnant of an essentially unrelated event.

The image on the cover highlights the role of noise in the generation of droplets. The experimental conditions (Re=861, We=673, H = 0.079) are such that secondary droplets would not ordinarily be produced. In this particular case, some initial inhomogeneity

Figure 10. *Left:* Crown splash without a microdroplet splash. Silicon oil, $\mathsf{Re} = 966$, $\mathsf{We} = 874$, $\mathsf{H} = 0.2$ at 200, 740, 1410, 2430 μs after impact. Corresponds to ▼ in Fig. 3. *Right:* Microdroplet splash without a crown splash. Glycerol/water mixture Re=1910, We=142, $\mathsf{H} = 0.2$ at 260, 940, 1780, 6880, 11200 μs after impact. Corresponds to ▲ in Fig. 3. Scale bar corresponds to 2 mm.

(probably a dust particle) disturbed the Peregrine sheet. The disturbance was amplified by the instability and two droplets were generated. We can reproduce the same structure by placing a small obstacle at the impact site. The sensitivity of drop generation on the initial conditions illustrates the difficulty of disentangling the instability of the ejecta sheet from the instability of the Peregrine sheet when the former interacts with the early stages of the latter.

Two more types of splashes are shown in Fig. 11. On the left we show a combination of small and large drops. The large drops come from the rim instability of the Peregrine sheet as described before, although the process is perhaps slightly more irregular. However, superimposed on this structure a number of much smaller drops are visible. These form from a horizontal sheet attached to the Peregrine sheet at early times.

The right hand side of Fig. 11 shows yet another phenomenon. The end of the Peregrine sheet may be significantly curved (also seen by [15]). We are not sure what causes this curvature but some possibilities are:

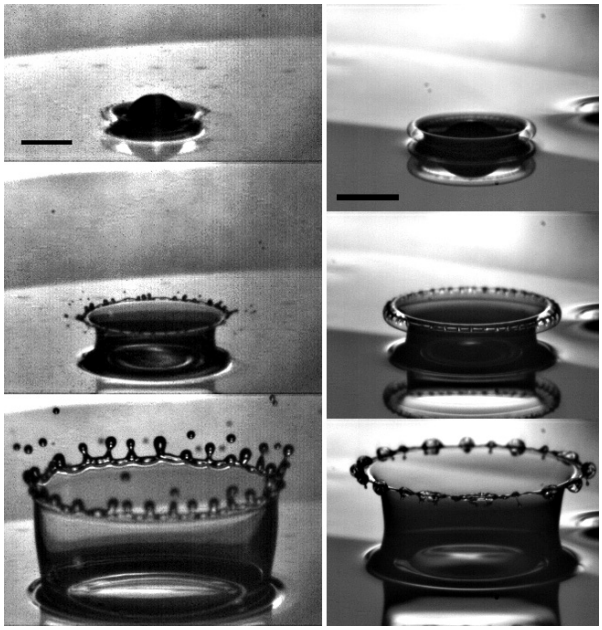

Figure 11. *Left:* Drop impact producing both a microdroplet and crown splash. Propanol Re=1816, We=582, H = 0.2 at 160, 570, 2650 μs after impact. Corresponds to ★ in Fig. 3. *Right:* Splash which entrains bubbles in to the Peregrine sheet rim. Silicon oil Re=1392, We=1326, H = 0.2 at 200, 610, 1010 μs after impact. Corresponds to ■ in Fig. 3. The scale bar corresponds to 2 mm.

(i) A time dependence of the ejection angle of the sheet [2]. The bending of the sheet may therefore be a purely kinematic effect.

(ii) The intrinsic dynamics of the sheet due to the action of surface tension, akin to the behaviour of an *elastic* sheet.

(iii) the effect of air.

In Fig. 11 the bending becomes so pronounced that the sheet closes in on itself, and bubbles are entrained, as seen in the last photograph of the sequence.

In summary, we have shown that there are at least three sources of secondary droplets:

(i) a prompt instability of the ejecta sheet which occurs immediately upon impact and produces very small droplets. Figure 8 shows an example of this splash.

(ii) a rim instability of the ejecta sheet which produces medium sized droplets. An example is given in Fig.11.

(iii) a rim instability of the Peregrine sheet which produces large droplets. This is referred to as crown splash in Fig. 3. The boundary of this regime follows the simple relationship $\mathsf{We} \cdot \mathsf{Re}^{0.5} = c$ with $c = 2.6 \times 10^4$, which agrees well with experimental observation as shown in Fig. 12. Curiously, the same correlation has been proposed in [18] for dry surfaces (but with a much smaller value of c), for which there is no Peregrine sheet. Similar correlations have also been found in [19]

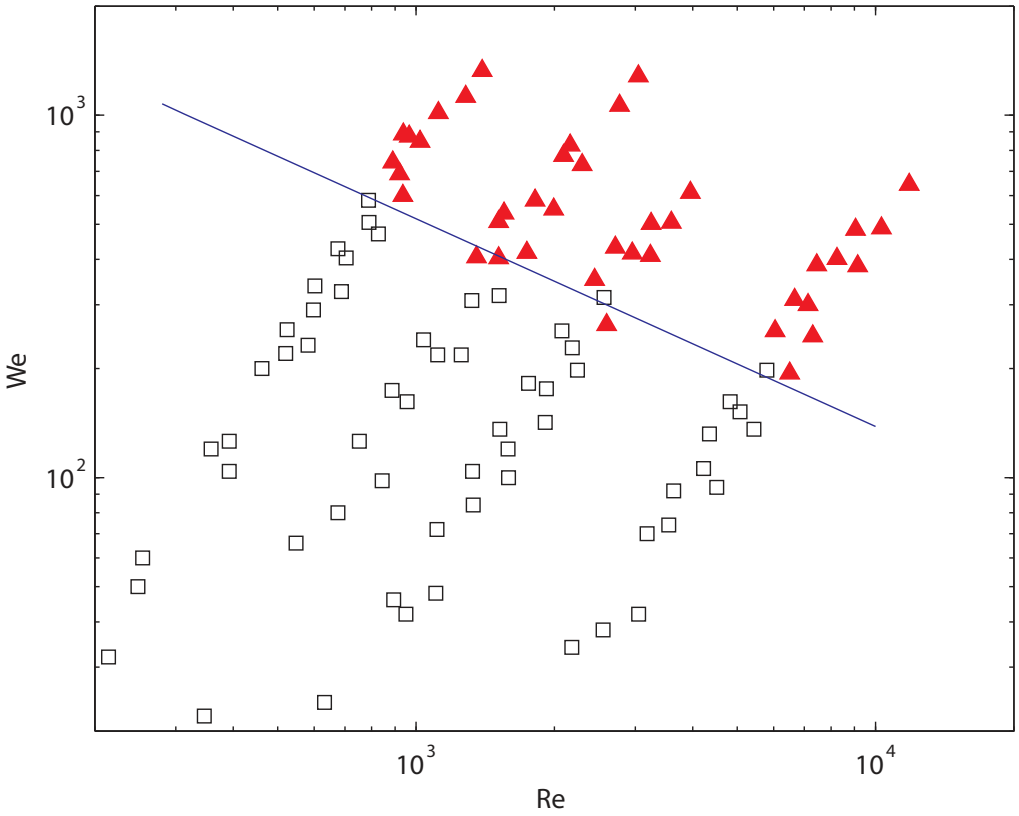

Figure 12. Drop impacts with (▲) and without (□) a crown splash. The solid line is a fit to the boundary using the power law $\mathsf{We} = c\ \mathsf{Re}^{-0.5}$, yielding $c = 2.6 \times 10^4$

for impact on thin films, but without specifying the mechanism by which drops are produced.

These mechanism are typically interdependent and with the earlier ones influencing the later ones. The phase diagram shown in Fig. 3, though still incomplete, reflects some of the complexities that arises from the interaction of these mechanisms.

Acknowledgments

Dedicated to our late colleague Howell Peregrine.

References

[1] Worthington A M 1908 *A Study of Splashes* (Longmans: London)
[2] Peregrine D H 1981 *J. Fluid Mech.* **106** 59
[3] Xu L, Barcos L and Nagel S R 2006 *arXiv:physics/0608079*
[4] Sikalo S, Wilhelm H D, Roisman I V, Jakirlic S and Tropea C 2005 *Phys. Fluids* **17** 062103
[5] Xu L, Zhang W W and Nagel S R 2005 *Phys. Rev. Lett.* **94** 184505
[6] Edgerton H E 1977 *Stopping time: the photographs of Harold Edgerton* (Abrams: New York)

[7] Josserand C and Zaleski S 2003 *Phys. Fluids* **15** 1650
[8] Yarin A L 2006 *Annu. Rev. Fluid Mech.* **38** 159–192
[9] Thoroddsen S T, Etoh T G and Takehara K 2006 *J. Fluid Mech.* **557** 63–72
[10] Bergeron V, Bonn D, Martin J Y and Vovelle L 2000 *Nature* **405** 772–775
[11] Rozhkov A, Prunet-Foch B and Vignes-Adler M 2006 *J. Non-Newtonian Fluid Mech.* **134** 44
[12] Kemp M 1998 *Nature* **396** 633
[13] Kadanoff L P 2000 *Univ. Chicago Record* **35** 2
[14] Vignes-Adler M 2004 Talk delivered at Euromech 450, Marseille
[15] Thoroddsen S T 2002 *J. Fluid Mech.* **451** 373
[16] Weiss D A and Yarin A L 1999 *J. Fluid Mech.* **385** 229
[17] Howison S D, Ockendon J R, Oliver J M, Purvis R and Smith F T 2005 *J. Fluid Mech.* **542** 1
[18] Mundo C, Sommerfeld M and Tropea C 1995 *Int. J. Multiphase. Flow* **21** 151
[19] Vander Wal R L, Berger G M and Mozes S D 2006 *Exp. Fluids* **40** 33